Supporting Information

The Tunable and Highly Selective Reduction Products on Ag@Cu Bimetallic Catalysts toward CO_2 Electrochemical Reduction Reaction

Zhiyuan Chang,[a] Shengjuan Huo,[a],[b],[c]* Wei Zhang,[a] Jianhui Fang,[a] Hailiang Wang[b],[c]*

*

[a] Department of Chemistry, Science Colleges, Shanghai University, 99 Shangda Road, Shanghai, 200444, China

[b] Department of Chemistry,Yale University, New Haven, Connecticut 06520, United States

[c] Energy Sciences Institute, Yale University, New Haven, Connecticut 06516, United States

E-mail: huoshengjuan@shu.edu.cn ; (S.H.);

hailiang.wang@yale.edu (H.W.).

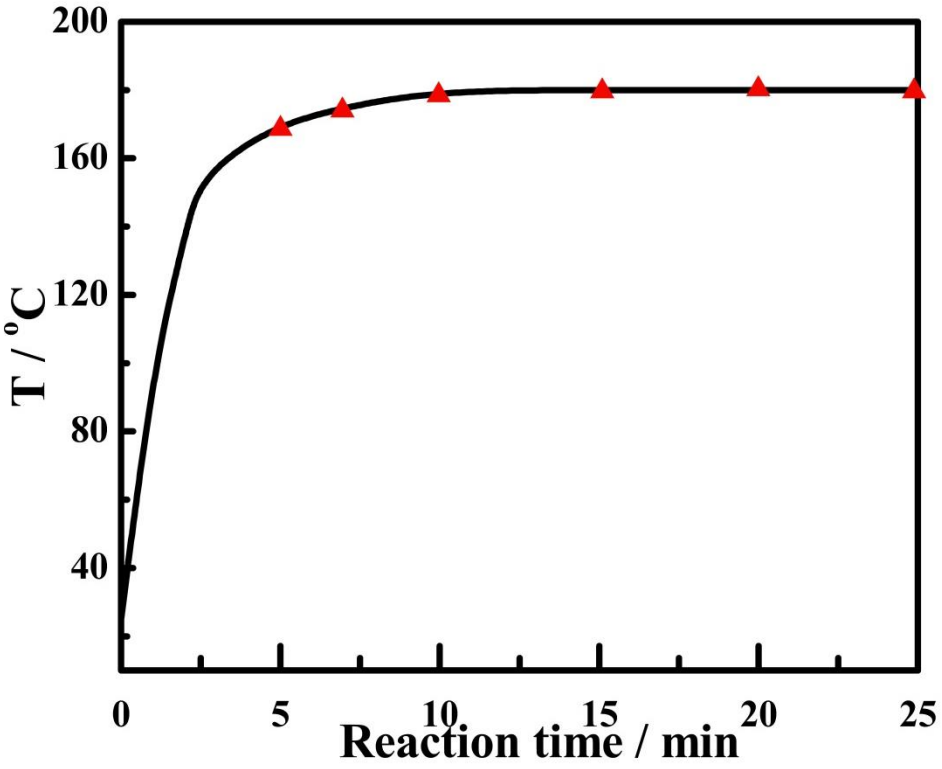

Figure S1. Temperature profile of reagent solution after injection of $AgNO_3$ / $Cu(OAc)_2 \cdot H_2O$ / PVP mixtures.

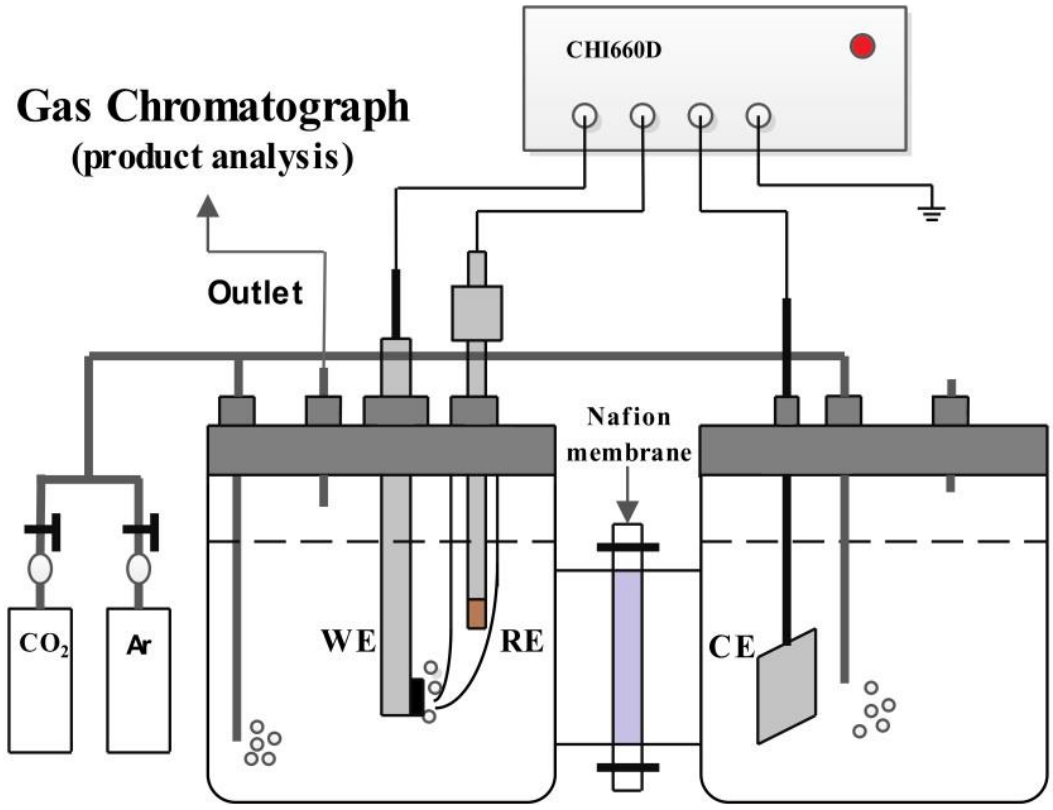

Figure S2. Schematic of the online electrochemical gas chromatograph (GC) system and home-made H-type electrochemical cell utilized in this work.

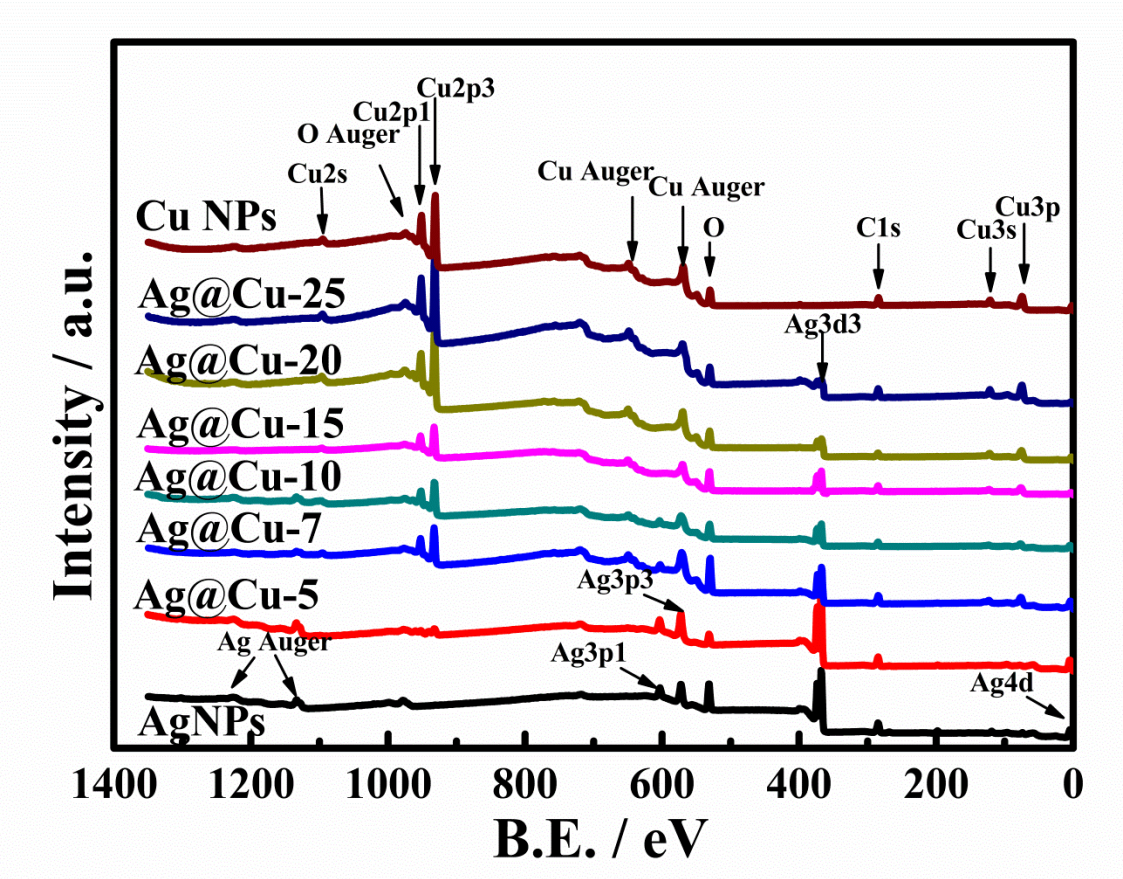

Figure S3. X-ray photoelectron survey spectra for Ag NPs, Cu NPs and the series of Ag@Cu bimetallic nanoparticles prepared at different reaction time.

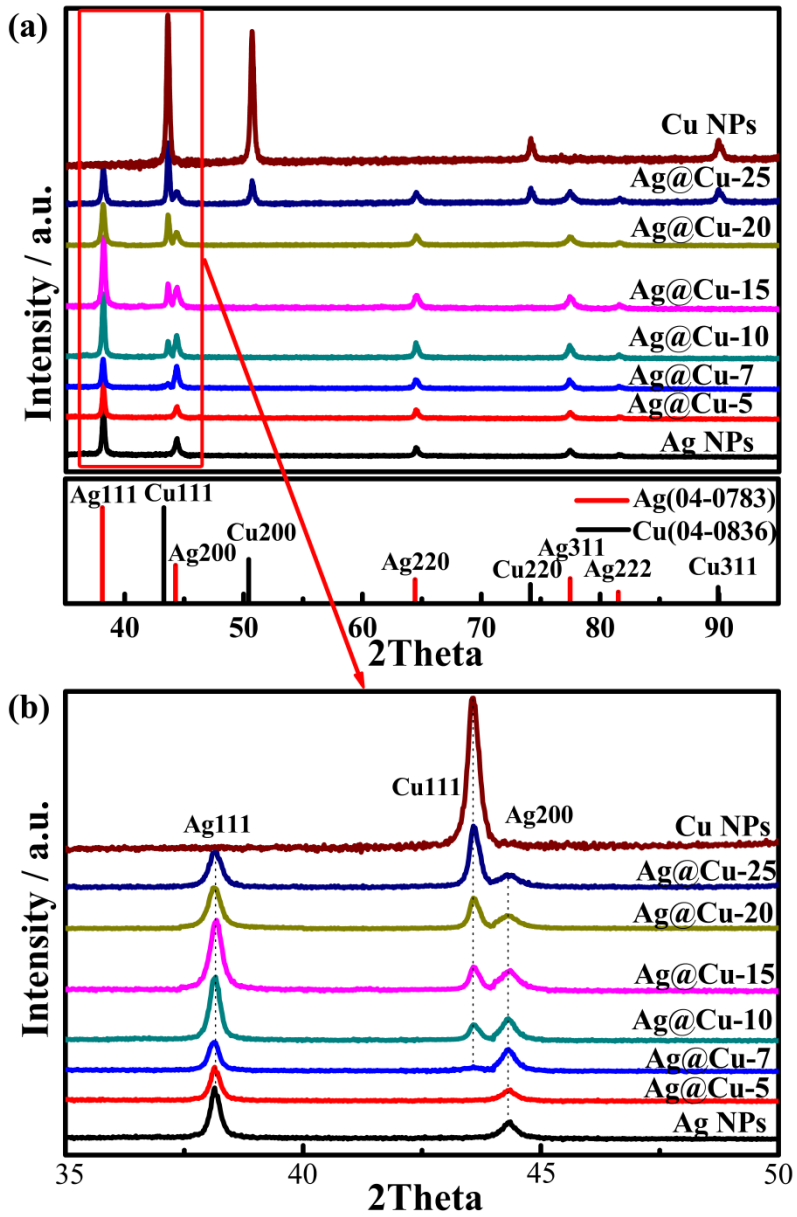

Figure S4. XRD patterns (a) and an enlarged XRD pattern (2theta from 35 to 50 degree) (b) of Ag NPs, Cu NPs and Ag@Cu bimetallic nanoparticles prepared at different reaction time.

X-ray diffraction (XRD) patterns were collected on D/MAX-2500V+/PC diffractometer (Rigaku Corporation, Japan) equipped with Cu-target X-ray tube and operated at 1800 watts. The data were recorded in the 2θ range between 10° and 95°.

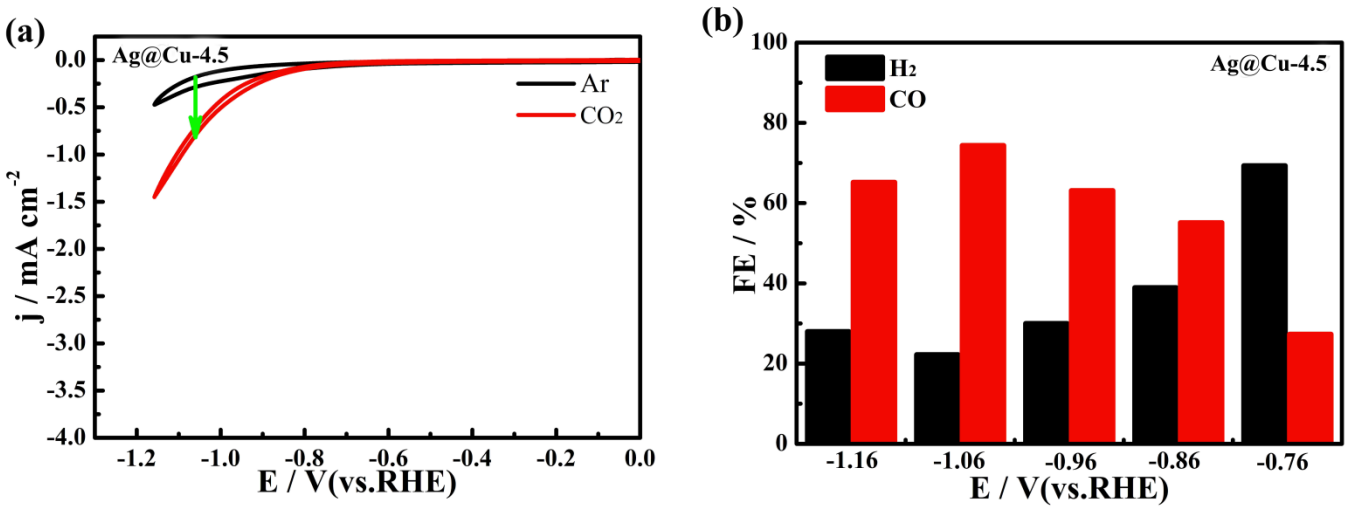

Figure S5. The CVs (a) and FEs of gaseous products (b) of Ag@Cu-4.5 electrocatalyst in 0.1 M $KHCO_3$ solution as a function of potential.

Table S1. Comparison of various Ag based electrocatalyst for CO or hydrocarbon-selective CO_2 reduction catalysts in the literature

Ref.	Material	Electrolyte	E	Faradaic efficiency (%)				Interaction (synergetic or dillution effects)*
				H_2	CO	CH_4	C_2H_4	
1	$Cu_{18}Ag_{82}$ alloy film	0.05M $KHCO_3$	-1.2 V (vs.SHE)	-	26	-	-	Synergetic effect
2	$Ag_{84}Cu_{16}$ dendrite catalyst	0.5 M $KHCO_3$	-1.06 V (vs. RHE)	50	35	-	-	Dillution effect
	Ag_{100} dendrite catalyst			13	64.6	-	-	N
3	$Cu_{28}Ag_{72}$ bulk alloy	0.1M $KHCO_3$	-0.55 V (vs.Ag/AgCl)	-	13	10	12	Synergetic effect
4	Au@Cu1 core–shell nanoparticles	PBS	-0.6 V (vs. RHE)	37	-	6	18	Synergetic effect
	Au@Cu2 core–shell nanoparticles			39		10	8	
	Au@Cu3 core–shell nanoparticles			50		18	3	N
5	Bulk Ag	0.1M $KHCO_3$	-1.05 V	18	88			N
6	$Ag/In(OH)_3$	0.1M KHCO	-0.6 V (vs. RHE)	35	51			Synergetic effect

7	AgCo	PBS	-1.2 V(vs. RHE	38.32	61.68		Synergetic effect

*Note: In terms of the AgCu bimetallic catalysts, we have listed the references concerning the studied alloy and surface galvanic materials for eCO2RR. Surprisingly, the two opposite points appeared in the reference, that was the CuAg bulk alloy for synergetic effects and galvanic Cu on Ag for dillution effects between Cu and Ag. As shown in ref.2, AgCu dendrite electrocatalysts showed the dilution effects in eCO2RR. Ag_{100} nanoparticle films was at the top of the volcano for CO_2 to CO, better than any bimetallic dendrite nanomaterials. However, as the opposite point, the synergistic effect can exist between the AgCu system. As for alloy materials, Watanabe's group reported the synergistic effect for CO on the electroplating Cu-Ag alloy film for CO_2RR. There appeared that the synergistic effect on the faradaic efficiency for CO product on the Cu-Ag alloy containing this large amount of Ag, and there was a maximum efficiency of 26% at -1.2 V (vs.SHE), which was larger than 8% and 2% on Cu and Ag electrodes, respectively. Nogami et al pointed that the Cu-Ag bulk alloy to the CO_2RR in a pulsed condition and found the selectivity to C_2 compounds. There also appears the synergistic effect on the faradaic efficiency for C_2 production on the Cu-Ag alloy and there is a maximum efficiency of 12% at -0.55 V (vs. Ag/AgCl) for the Cu/Ag 28/72 electrode. In regard to Ag and other materials such as In, Co, the FE for CO are 51 and 68%, respectively. However, the Ag bulk or different Ag nanoparticles in structure, size, morphology, oxidation state et al,[8] the FE for CO varied and the highest FE could reach as high as 92% at -0.9 V vs. RHE.

No Ag@Cu bimetallic core-shell structured electrocatalysts can be referred. However, in Monz´o et al's work, Au@Cu core-shell nanoparticles with well-defined surface structures were synthesized and evaluated as catalysts for the eCO_2RR in neutral medium. They observed that the Au cubic nanoparticles with 7–8 layers of copper present higher selectivity toward the formation of ethylene (FE≈18%) in PBS (pH = 8) at -0.6 V (vs. RHE). Compared with Au@Cu catalyst, Ag@Cu electrocatalyst in our case can have ca. 29% ethylene FE.

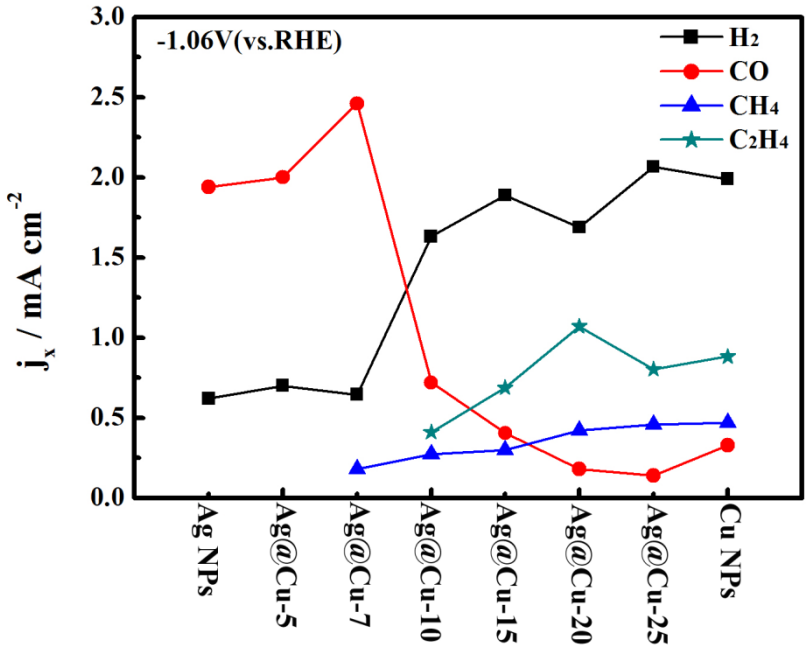

Figure S6. Partial current densities j_x of H_2, CO, CH_4, C_2H_4 for the series of the electrocatalysts at -1.06 V (vs. RHE) in 0.1 M $KHCO_3$

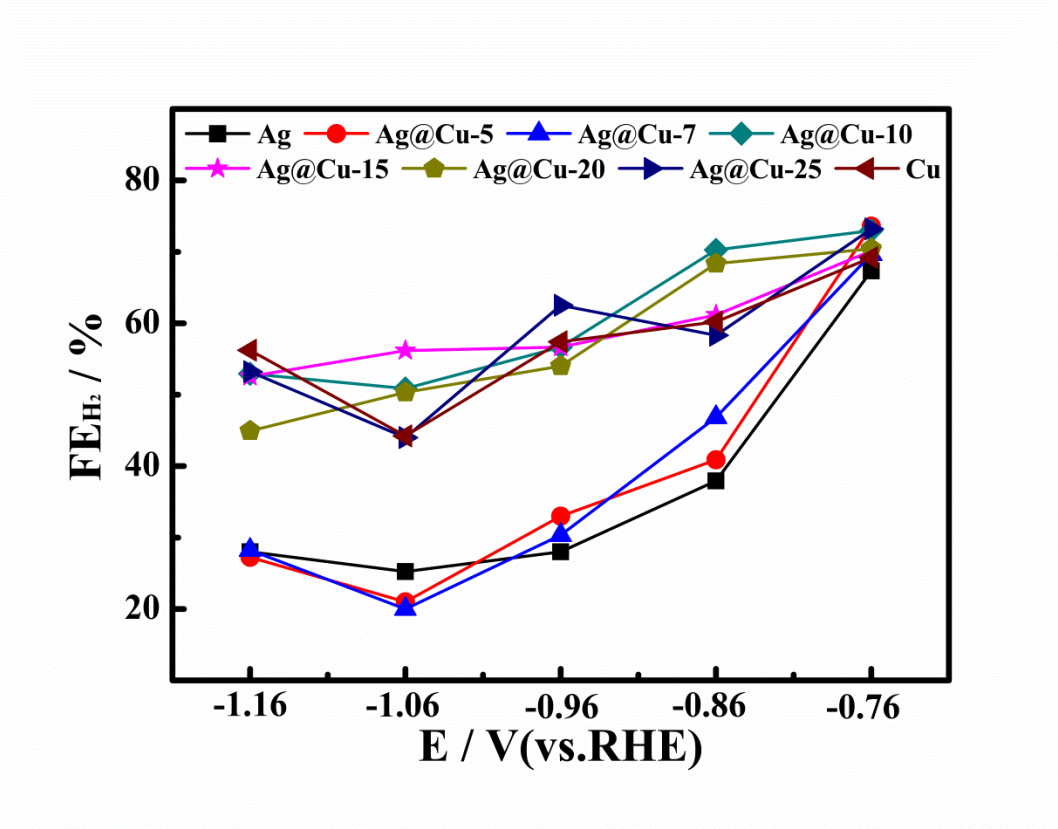

Figure S7. Comparison of potential dependent FEs for H_2 on different electrocatalysts.

Figure S7 summarized the trends of H_2 in FEs dependent on the applied potentials for different Ag@Cu electrocatalysts. As what was illustrated, the FEs of H_2 both increased with more negative applied potentials as well as copper content in electrocatalysts overall. At the same applied potentials with higher overpotentials, Cu catalysts produced more H_2 than Ag catalysts mainly due to its nature in metallic structure. Nearly double times of H_2 production was observed for Cu as active center on the surface of the core-shell structured catalysts. It meant that reactions about H^+ (aq) $+e^-$ + * $\rightarrow$H * or *+H (aq)$+e^-\rightarrow H_2$+* could be easily occured on Cu surface.

However, at the lower overpotentials, these eight catalysts had the similar FEs for H_2. It was probably because the electron transfer reaction was the limited step at the lower overpotential for H_2 formation.

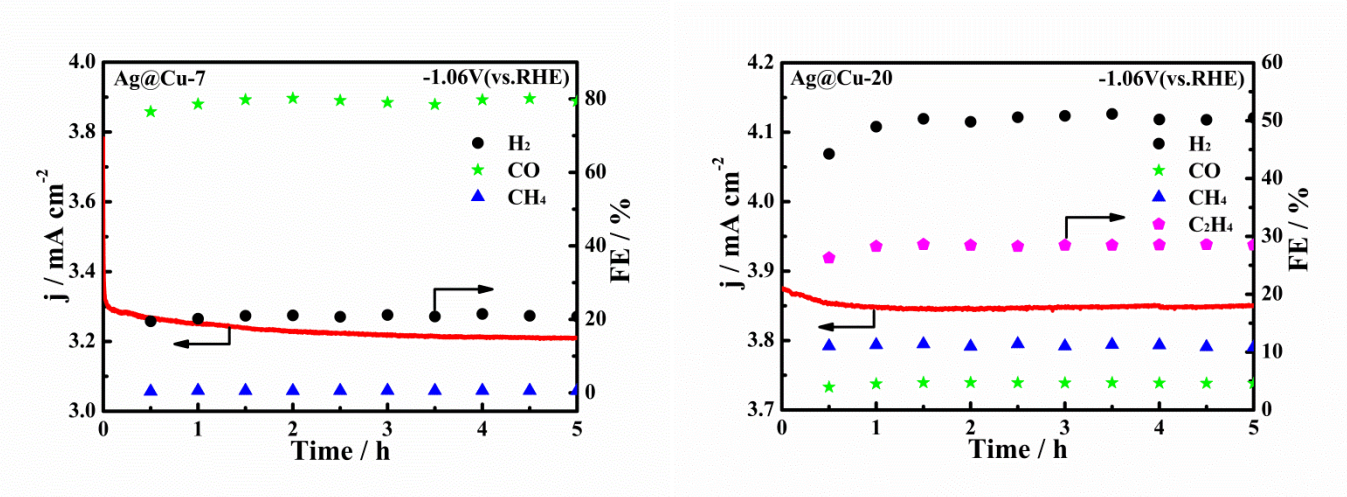

Figure S8. Total current density (left axis) and Faradaic efficiency for each gaseous product(right axis) of Ag@Cu-7(left column) and Ag@Cu-20 (right column) as a function of time, measured in CO_2-saturated 0.1 M $KHCO_3$ at −1.06 V (vs. RHE).

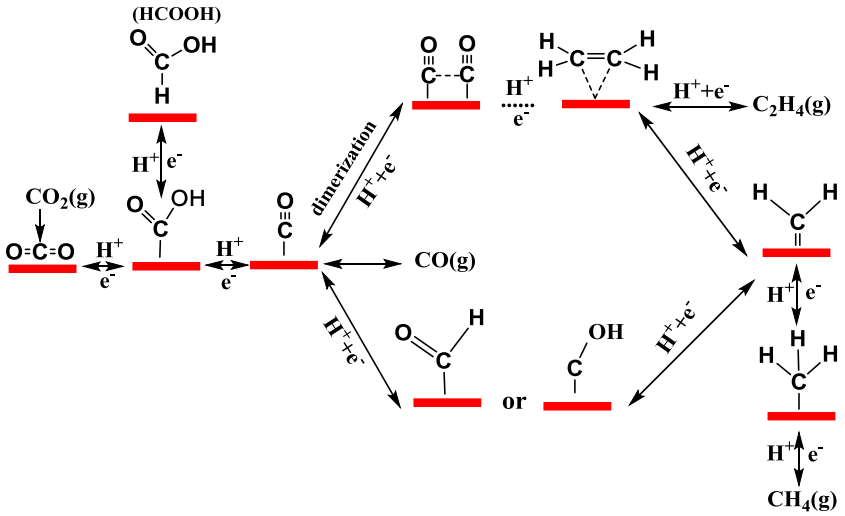

Scheme S1. The possible scheme for CO_2 electroreduction reaction on surfaces of the electrocatalysts .[5,9]

REFERENCES

(1) Watanabe, M.; Shibata, M.; Kato, A., Design of Alloy Electrocatalysts for CO_2 Reduction. *J. Electrochem. Soc.* **1991**, 138, 3382-3389.

(2) Choi, J.; Kim, M. J.; Ahn, S. H.; Choi, I.; Jang, J. H.; Ham, Y. S.; Kim, J. J.; Kim, S.-K., Electrochemical CO_2 Reduction to CO on Dendritic Ag–Cu Electrocatalysts Prepared by Electrodeposition. *Chem. Eng. J.* **2016**, 299, 37-44.

(3) Ishimaru, S.; Shiratsuchi, R.; Nogami, G., Pulsed Electroreduction of CO_2 on Cu-Ag Alloy Electrodes. *J. Electrochem. Soc.* **2000**, 147, 1864-1867.

(4) Vidal-Iglesias, J. ; Solla-Gullón,J. ; Koper, M. T. M. ; Rodriguez P., Shape-Templated Growth of Au@Cu Nanoparticles. *J. Mater. Chem. A* **2015**, 3, 23690-23698.

(5) Hatsukade, T.; Kuhl, K. P.; Cave, E. R.; Abram, D. N.; Jaramillo, T. F., Insights into the Electrocatalytic Reduction of CO_2 on Metallic Silver Surfaces. *Phys. Chem. Chem. Phys.* **2014**, 16, 13814-13819.

(6) Larrazábal G. O.,Matín A. J., Mitchell S.; Hauert R., Pérez-Ramírez J., Synergistic effect in silver-indium electrocatalysts for carbon dioxide reduction, *J. Catal.* **2016**, 343, 266-277.

(7) Singha, S. ; Gautamb, R. K.; Malikb, K.; Verma, A. , Ag-Co bimetallic catalyst for electrochemical reduction of CO_2 to value added products, J. CO_2 Utiliz. **2017,** 18 , 139–146 .

(8) Ma, M.; Trzésniewski, B. J.; Xie, J.; Smith, W. A.; Selectivity and Efficient Reduction of Carbon Dioxide to Carbon Monoxide on Oxide-Derived Nanostructured Silver Electrocatalysts, *Angew. Chem. Int. Ed.* **2016**, 55, 9748-9758.

(9) Kuhl, K. P.; Cave, E. R.; Abram, D. N.; Jaramillo, T. F., New insights into the electrochemical reduction of carbon dioxide on metallic copper surfaces, *Energy Environ. Sci.* **2012**, 5, 7050-7059.